MOLECULAR AND CELLULAR BIOLOGY, Dec. 1996, p. 6698–6706 Vol. 16, No. 12
0270-7306/96/$04.00+0

Two Human cDNAs, Including a Homolog of *Arabidopsis FUS6* (*COP11*), Suppress G-Protein- and Mitogen-Activated Protein Kinase-Mediated Signal Transduction in Yeast and Mammalian Cells

BRIAN H. SPAIN, KATHERINE S. BOWDISH, ADAM R. PACAL, SUSANNE FLÜCKIGER STAUB, DERRICK KOO, CHIA-YUAN R. CHANG, WEILIN XIE, AND JOHN COLICELLI*

Department of Biological Chemistry and Molecular Biology Institute, UCLA School of Medicine, Los Angeles, California 90095

Received 5 March 1996/Returned for modification 22 April 1996/Accepted 3 September 1996

We have isolated two novel human cDNAs, *gps1-1* and *gps2*, that suppress lethal G-protein subunit-activating mutations in the pheromone response pathway of the yeast *Saccharomyces cerevisiae*. Suppression of other pathway-activating events was examined. In wild-type cells, expression of either *gps1-1* or *gps2* led to enhanced recovery from cell cycle arrest induced by pheromone. Sequence analysis indicated that *gps1-1* contains only the carboxy-terminal half of the *gps1* coding sequence. The predicted gene product of *gps1* has striking similarity to the protein encoded by the *Arabidopsis FUS6* (*COP11*) gene, a negative regulator of light-mediated signal transduction that is known to be essential for normal development. A chimeric construct containing *gps1* and *FUS6* sequences also suppressed the yeast pheromone pathway, indicating functional conservation between these human and plant genes. In addition, when overexpressed in mammalian cells, *gps1* or *gps2* potently suppressed a RAS- and mitogen-activated protein kinase-mediated signal and interfered with JNK activity, suggesting that signal repression is part of their normal function. For *gps1*, these results are consistent with the proposed function of *FUS6* (*COP11*) as a signal transduction repressor in plants.

In eukaryotes, heterotrimeric G proteins are essential for cellular responses to diverse external stimuli, including pheromones, hormones, growth factors, odorants, and light. In each case, the G protein is coupled to a seven-transmembrane receptor. Upon ligand binding, the activated receptor causes dissociation of the G protein into a Gβγ heterodimer and a free GTP-bound Gα subunit. In mammalian cells, both Gβγ and Gα can interact with a variety of effector proteins that can subsequently control second-messenger production, transcription, cell cycle progression, and differentiation (reviewed in reference 41).

In the yeast *Saccharomyces cerevisiae*, the pheromone response pathway is regulated by a heterotrimeric G protein and a mitogen-activated protein (MAP) kinase cascade (reviewed in references 2, 27, 44, and 53). The resulting signal causes cells to arrest in late G_1 and to differentiate. Morphologically altered cells (shmoos) of opposite mating type can attach and fuse, leading to mating resolution and resumption of mitotic growth as a diploid. If mating is not consummated, haploid cells undergo adaptation and return to normal growth.

Binding of pheromone from one haploid mating type to its cognate receptor expressed on a haploid cell of the opposite mating type triggers activation of a receptor coupled G protein by releasing the Gα subunit (encoded by the *GPA1* [*SCG1*] gene) from the signal transducing Gβγ heterodimer (encoded by *STE4* and *STE18*, respectively). Downstream effectors include the *STE20*-encoded protein kinase (33, 50), which is structurally related to mammalian Pak kinase (36). Ste20p activates a series of kinases composed of the products of the *STE11*, *STE7*, *FUS3*, and *KSS1* genes. This grouping of protein kinases is referred to as a MAP kinase cascade based on its striking structural similarity to ordered series of mammalian MAP kinases (e.g., Raf-MEK-ERK and MEKK-JNKK-JNK) that are stimulated by the small G protein RAS (39) and may also be activated by heterotrimeric G proteins (15, 26, 38, 60). In *S. cerevisiae*, some Gβγ signaling properties may derive from a direct interaction with Ste5p (65), a scaffold protein that physically coordinates the yeast MAP kinase cascade (11). Further downstream, the transcription factor Ste12p induces genes, such as *FUS1*, that are required for mating. Many of these pheromone signaling components are also known to participate in parallel but distinct pathways (reviewed in references 22, 27, and 34).

Elimination or functional impairment of Ste proteins causes a block in the pheromone response pathway and leads to a sterile (*ste*) phenotype. Some mutations in pheromone signaling elements can result in a constitutive signal that, even in the absence of pheromone, leads to differentiation and cell cycle arrest. Such mutations include deletion of the Gα subunit (17, 40), overexpression of the Gβ subunit (12), expression of a mutant Gβ subunit that has reduced affinity for Gα (4, 64), constitutively active Ste20p (50), constitutively active Ste11p (7, 57), and overexpressed Ste12p (20). We have isolated human cDNAs as high-copy-number suppressors of a constitutively active Gβγ heterodimer in yeast. One of these suppressors, *gps1-1*, is a truncated form of *gps1* which is highly related structurally and functionally to the *Arabidopsis FUS6* (*COP11*) gene, a negative regulator of photomorphogenic signaling (5). G-protein–MAP kinase pathway activation events in yeast and mammalian cells were used to probe the functions of *gps1* and *gps2*.

MATERIALS AND METHODS

Strains, media, and suppression assays. Yeast strains LG2TG (*MAT*α *ade8 his3 leu2 trp1 ura3 can1 gpa1*::*HIS3* pTGC) and DBC (*MAT***a** *ade2 ade3 his4 leu2 lys2 trp1 ura3 cry1 can1 SUP4-3 STE4^{Hpl}* pUα2C) were previously described (56).

* Corresponding author. Phone: (310) 206-7800. Fax: (310) 206-5272. Electronic mail address: colicelli@biochem.medsch.ucla.edu.

LG2TG cells were transformed with a human glioblastoma cDNA library (14), and *gpa1* suppressors were isolated by plasmid exchange selection as previously described (56) except that one round of enrichment was required in order to isolate individual suppressors. Survivors of the first selection were pooled, and plasmid DNA isolated from these cells was used to transform fresh LG2TG cells that were then subjected to plasmid exchange selection. Resulting survivors were then analyzed individually. Suppression analysis of the $STE4^{Hpl}$ mutation in strain DBC has been previously described (56). Viability and *FUS1*::*lacZ* induction assays using plasmid-borne pathway activators were performed in strain AN43-5A (*MAT***a** *ade1 arg4 leu2 trp1 ura3 mf***a***1*::*FUS1*::*lacZ his3*::*FUS1*::*HIS3* [49]; generously provided by Ira Herskowitz, University of California, San Francisco). The W303-1A/1B diploid (*MAT***a**/*MAT*α *ade2*/*ade2 his3*/*his3 leu2*/*leu2 trp1*/*trp1 ura3*/*ura3 can1*/*can1*) was generated from W303-1A and W303-1B strains provided by Rodney Rothstein. For the viability assays, pathway activator plasmids used were pM4GT (vector control), YCpGal-STE4, pM4GT-STE20ΔN, pKB254 (pGAL-STE11ΔN), and pGK40 (pGAL-STE12). Suppressor plasmids used were pYES2 (vector control), pKB247 (pGAL-gps1-1), pKB241 (pGAL-gps2), and pYESS-MSG5. Individual transformants were streaked onto the appropriate selective media containing sucrose. These were replica plated to either sucrose or galactose media. Growth was scored at 3 days. *FUS1*::*lacZ* inductions were done essentially as described previously (37) except that cultures were normalized to the same optical density at 600 nm prior to induction. The plasmids used in the *FUS1*::*lacZ* induction experiments were as follows. For the experiments using *STE4*, *STE11ΔN*, and *STE12* as the activating signals, expression plasmids YCpGAL-STE4, pKB254, and pGK40, respectively, were used. In these experiments, pKB247, pKB241, pYESS-MSG5, and pUG were the suppressor candidates; pYESS was the vector control. For the experiments using *STE20ΔN* as the activating signal, pYESS-STE20ΔN was used for testing the suppression candidates expressed from pM4GT-gps1-1, pM4GT-gps2, and pM4GT-MSG5; pM4GT was the vector control. pM4GT-STE20ΔN was used for testing *GPA1* (pUG) as the suppressor candidate; pYESS was the vector control. β-Galactosidase assays were done as described previously (56). Halo assays were performed as previously described (56), using strains SP1 (*MAT***a** *ade8 his3 leu2 trp1 ura3 can1*), GPY74-15Ca (*MAT***a** *his4* or *his6 leu2 trp1 ura3 sst1*) (58), and YDM400 (*MAT***a** *ade2 his3 leu2 lys2 trp1 ura3 sst2*), which was generously provided by Doreen Ma and Jeremy Thorner, University of California, Berkeley. The amount of α-factor used was 20 μg (wild-type cells) or 2 μg (*sst1* and *sst2* cells). Morphological analysis of pheromone-treated cells was done as follows. GPY74-15Ca cells transformed with pADANS, p19A, or p17B were inoculated with 5×10^5 cells per ml. After 1 h in culture, α-factor was added to achieve a final concentration of 1 μg/ml. Every 30 min over a 3-h period, aliquots were mixed with an equal volume of fixing solution (150 mM NaCl, 7.4% formaldehyde), and at least 200 cells were examined microscopically. For the pheromone withdrawal experiment, cells previously treated with pheromone for 3 h were washed twice and then cultured in pheromone-free media. Aliquots were removed every hour for 5 h and treated as described above.

Plasmid constructions. The *gps1-1* and *gps2* cDNA library isolates, expressed as Adh1p fusions, were designated p19A and p17B, respectively. The hemagglutinin (HA)-tagged constructs of *gps1-1* (pKB224) and *gps2* (pKB222) were created by subcloning the *Not*I cDNA fragments from p19A and p17B into a modified form of pAD54N (48). The HA-tagged full-length form of *gps1* (pKB226) was made from an isolate (clone 9-1) derived from a human brain cDNA library (Clontech) and subcloned into pBluescript (Stratagene). The 9-1 clone was first modified by PCR amplification of the 5′ end, introducing a *Sal*I restriction site upstream of the initiation codon. This 5′-end fragment (*Sal*I to *Apa*I) was then ligated with the *Apa*I-to-*Not*I fragment of the 9-1 clone into pAD54N in a three-way ligation. The shorter construct that initiates with a downstream ATG was made by directly cloning a shorter cDNA isolate (clone 6-1), using *Hin*dIII and *Sac*I, into the pAD54-related plasmid pAD4 (13). The *gps1-1ΔC1* deletion (pKB237) was generated by digesting p19A with *Pst*I and ligation to an adapter oligonucleotide that destroys this site and generates a stop codon. For *gps1-1ΔC2*, the entire p19A *gps1-1* insert was moved as a *Not*I fragment into pBluescript (pKS19). This construct was then digested with *Nsi*I and ligated to the same adapter oligonucleotide as above to introduce an early stop codon (pKB238). The entire *Not*I fragment was then cloned back into pADANS, the original library vector, to give pKB240. The internal deletion (pKB252) was generated by ligation of the *Not*I-to-*Pst*I fragment and the *Nsi*I-to-*Sac*II fragment of p19A together with *Not*I- and *Sac*II-digested pADANS vector in a three-way ligation resulting in a deletion of sequence between *Pst*I and *Nsi*I (these sites are in the same reading frame). YEpGPA1 was made by inserting the *Eco*RI genomic fragment of *GPA1* into YEp13M4 (partially *Eco*RI digested). pUG was made by inserting the *Eco*RI fragment of *GPA1* into pUV2, a 2μm-based *URA3* marked plasmid which was a generous gift of Junichi Nikawa and Michael Wigler.

The *FUS6* cDNA was amplified from an *Arabidopsis* (strain WS) silique cDNA library (63) generously provided by John Harada, University of California, Davis. Independent clones derived from duplicate PCRs were used, and these always behaved identically. *FUS6ΔN* clones were also derived from PCR amplification using an upstream primer that introduces an initiator codon at position 1228 of *FUS6* (8). Again, independent clones were generated. Full-length and truncated *FUS6* were expressed from epitope fusion (pAD54) and nonfusion (pADNS [13]) yeast vectors.

The chimeric *gps1*:*FUS6* clone (pKB251) was constructed from four fragments in sequential ligations. The 5′ portion is a PCR-generated *Not*I-to-*Hin*dIII fragment of *gps1-1* in which the *Hin*dIII site was artificially introduced at position 943. The central portion is a PCR-generated *Hin*dIII-to-*Nsi*I fragment of *FUS6* in which the *Nsi*I site was artificially introduced at position 1064. The 3′ portion is an *Nsi*I-to-*Sac*II fragment of *gps1-1* taken directly from p19A. The resulting chimera was expressed from the pADANS library vector.

GAL promoter constructs of *gps1-1* (pKB247) and *gps2* (pKB241) with a *URA3* marker (*STE4*, *STE11ΔN*, and *STE12* experiments) were made by first moving the *Not*I fragments of *gps1-1* or *gps2* into pYES2 (Invitrogen, Inc.). In each case, the Adh1 fusion peptide originally present in the library isolates was incorporated into the new *GAL* constructs, using PCR amplification and subcloning. The *LEU2*-marked expression constructs regulated by the *GAL10* promoter were made by ligating PCR-amplified inserts into pM4GT, which was made by first moving the blunt/*Pst*I GAL_{UAS} fragment of pKB253 into YEp13M4 (42). The blunt terminus for the GAL_{UAS} insert was created by *Bam*HI digestion and Klenow enzyme treatment. The blunt terminus of YEp13M4 was created with *Hin*dIII and Klenow enzyme. The *ADH1* transcription terminator signal from pADHSN was moved as a *Bam*HI/*Sal*I fragment into the above-ligated product, thereby creating pM4GT. pKB253 was made in two steps. First, the *Eco*RI/*Sal*I fragment from pBM150 (30) was subcloned into pBluescript. From this, the *Sac*I/*Sal*I fragment was moved into YEp13M4. pADHSN was created by using an oligomeric adapter which changed the *Hin*dIII site of pADNS into a *Sal*I site. To create pM4GT-gps1-1 and pM4GT-gps2, PCR amplicons were cloned into pM4GT as *Sal*I/*Sfi*I fragments. The original library isolates were used as templates. The upstream PCR primer hybridized to the Adh1p fusion of the original clones and introduced an in-frame *Sal*I site. The downstream primer hybridized to the *ADH1* terminator prior to an *Sfi*I site. To create pM4GT-MSG5 and pYESS-MSG5, *MSG5* was PCR amplified and the resulting PCR product was cloned as a *Sal*I/*Not*I fragment into pADHSN. A functional clone was subsequently moved as a *Sal*I/*Not*I fragment into pM4GT and pYESS. pYESS was created by changing the *Hin*dIII site of pYES2 to a *Sal*I site, using an oligonucleotide adapter.

The genetic suppression and localization analysis utilized *GAL1/10* promoter-driven constructs of *STE4* (YCpGAL-STE4 [12], generous gift of Steven Reed, Scripts Research Institute), *STE11ΔN* (YGL-STE11ΔN [7], generous gift of Roger Kornberg, Stanford University), and *STE12* (pGK40 [68], generous gift of Stanley Fields, University of Washington). To make pKB254, the *Eco*RI-to-*Xba*I fragment containing *STE11ΔN* from YGL-STE11ΔN was first subcloned into pBluescript with a *GAL1/10* promoter sequence derived from pBM150. A *GAL* promoter-driven *STE11ΔN* fragment (*Sal*I-*Sac*I) was then moved into YEp13M4 to yield pKB254. Two pGAL-STE20ΔN constructs were made: pYESS-STE20ΔN with a *URA3* marker and pM4GT-STE20ΔN with a *LEU2* marker. *STE20ΔN* was PCR amplified by using an upstream primer that introduces a *Sal*I site prior to codon 495 and a downstream primer that introduces a *Not*I site. The resulting PCR products were cloned as *Sal*I/*Not*I fragments into pYESS. A functional clone was subsequently moved as a *Sal*I/*Not*I fragment into pM4GT.

Mammalian cell expression constructs were created by first PCR amplifying HA-tagged full-length *gps1* from pKB226 and inserting this into the *Bam*HI site of pcDNA3 (Invitrogen). The *gps1-1* and *gps2* constructs were generated by substituting *Not*I fragments from pKB224 and pKB222, respectively. Deletion of a *Not*I insert generated an empty HA-tagged vector (pcDNA3-HA) used in the control experiments.

Northern (RNA) blot and Western blot (immunoblot) analyses. Northern blot analyses were performed with Multiple Tissue Northern filters (Clontech). Equalized sample loading was analyzed by hybridization with an actin probe. For protein analysis, cells were grown to saturation in plasmid selection medium, transferred to YPD (rich medium), grown from optical density at 600 nm of 0.2 to 0.5, harvested, and lysed with glass bead treatment. One hundred micrograms of total protein was loaded per lane, and low-range prestained markers (Bio-Rad) were used. The HA antibody 12CA5 was used (43), and the blots were developed with alkaline phosphatase-conjugated goat anti-mouse antibody and 5-bromo-4-chloro-3-indolylphosphate toluidinium color reagent (Bio-Rad).

Mammalian cell transfections and assays. Procedures for $CaPO_4$-mediated transfections and luciferase assays have been previously described (66). In all transfections, including titrations, total DNA per transfection was held constant by adjusting the relative amounts of empty vector and suppressor plasmid used. The dominant negative *ras* allele H-ras^{Asn17} (6) was expressed from pZIPN17 (Geoffrey Cooper, Harvard University). The pcDNA3-HAgps1, pcDNA3-HAgps2, and pcDNA3-HA vector DNA samples were purified by CsCl gradient centrifugation. The immunocomplex JNK1 assays were performed essentially as described previously (67) except that the cells were harvested 18 to 22 h after transfection and the lysates were precleared with 20 μl of immobilized protein A (Pierce) prior to the addition of the Protein G Plus (Oncogene Science)-coupled M2 antibody (Eastman Kodak Co.) that recognizes the amino-terminal Flag tag on JNK1. Kinase activity assays using a glutathione *S*-transferase (GST)–c-Jun(1-79) substrate were quantitated with a PhosphorImager (Molecular Dynamics) and normalized to total protein. The assay was independently performed three times with the same result. Flag-JNK1 and GST–c-Jun(1-79) plasmids were from Roger Davis (University of Massachusetts Medical School).

Nucleotide sequence accession numbers. GenBank accession numbers for *gps1* and *gps2* are U20285 and U28963, respectively.

RESULTS

Isolation of human cDNAs that suppress the yeast *gpa1* mutation. To identify human proteins that affect G-protein–MAP kinase signaling, we selected for cDNAs that suppress the lethality resulting from a *gpa1* (Gα deficiency) mutation in yeast. We used a *gpa1* mutant strain (LG2TG) which harbors a maintenance plasmid, pTGC, that has a wild-type *GPA1* gene, a positive selectable marker (*TRP1*), and a negative selectable marker (*CAN1*). These cells were transformed with a human glioblastoma cDNA library in a high-copy-number yeast vector carrying a selectable marker (*LEU2*). Expression was driven by the yeast alcohol dehydrogenase (*ADH1*) promoter with the incorporation of an amino-terminal Adh1 peptide (14). Suppressors were obtained by using a modified plasmid exchange protocol (56). Transformants were grown for 2 days in liquid media, selecting for the library plasmid only. These cells were then plated on medium selective for retention of the library plasmid but loss of the pTGC maintenance plasmid (SC-leucine-arginine with canavanine). Colonies were then pooled and used to prepare DNA enriched for suppressor plasmids. This DNA was used to transform fresh LG2TG cells, and the same selection was performed, yielding individual colonies from which clonal library plasmid DNA was obtained. From approximately 10^7 transformants analyzed, five *gpa1* suppressors were isolated (Fig. 1A). Three of these encoded human Gsα. It has been previously reported that this structurally related protein is a functional homolog of yeast Gpa1p (17). The remaining two plasmids contained novel human cDNA sequences, designated *gps1-1* and *gps2* (G-protein pathway suppressor), that can suppress *gpa1* lethality in both mating-type backgrounds (data not shown).

Genetic localization of pathway suppression by *gps1-1* and *gps2*. Constitutive pheromone signaling can be mimicked by direct activation of the Gβ subunit. We tested the abilities of *gps1-1* and *gps2* to rescue the lethality of cells carrying a $STE4^{Hpl}$ mutation (4). This leads to constitutive signaling due to a reduced affinity for Gα (64). In a plasmid exchange and selection assay (56), both *gps1-1* and *gps2* were shown to suppress this lethal signal (Fig. 1B). Consistent with these data, *gps2* (and to a much lesser extent *gps1-1*) as well as overexpressed Gα (*GPA1*) were able to suppress *FUS1* induction arising from overexpressed *STE4* (Table 1). Each suppressor was also capable of suppressing the long-term lethal effects of overexpressed *STE4* (data not shown). These results prompted us to explore the effects of *gps1-1* and *gps2* on downstream signaling mutants.

We tested the abilities of *gps1-1* and *gps2* to suppress constitutively active forms of *STE20* (50), *STE11* (7), and overexpressed *STE12* (20). Unremitting signals from these pheromone pathway elements could not be blocked sufficiently to reverse their lethal effects (data not shown). It should be noted, however, that *STE20*Δ*N*-mediated lethality occurs even in cells with a defective pheromone pathway (50) and that *STE20*Δ*N*, *STE11*Δ*N*, and high-copy-number *STE12* were each lethal in diploid cells (Fig. 1C) which do not express some pheromone pathway components, including the G-protein subunits, Ste5p and Fus3p (reviewed in reference 27). In contrast, *STE4* overexpression is not lethal in diploids (Fig. 1C). These data suggest that the lethal phenotypes of *STE20*Δ*N*, *STE11*Δ*N*, and overexpressed *STE12* may involve some signal(s) other than the pheromone response pathway.

To circumvent the limitations of the lethal phenotype mapping experiments, we examined what effects these suppressors would have on pheromone pathway-specific signaling by monitoring *FUS1* induction. Consistent with the observed suppression of *STE4*-mediated induction (Fig. 1B), *gps2* was capable of interfering with *STE4*-induced *FUS1*::*lacZ* activity whereas *gps1-1* had only a slight inhibitory effect (Table 1). *gps1-1* did not interfere with *STE20*Δ*N*-, *STE11*Δ*N*-, and overexpressed *STE12*-mediated activation of the *FUS1*::*lacZ* reporter. Conversely, *gps2* blocked each of these signals by 30%. As expected, *GPA1* overexpression blocked only the overexpressed *STE4*-mediated signal and had no effect on downstream activators. Another control repressor used was *MSG5*, which encodes a phosphatase that can downregulate Fus3p kinase (19)

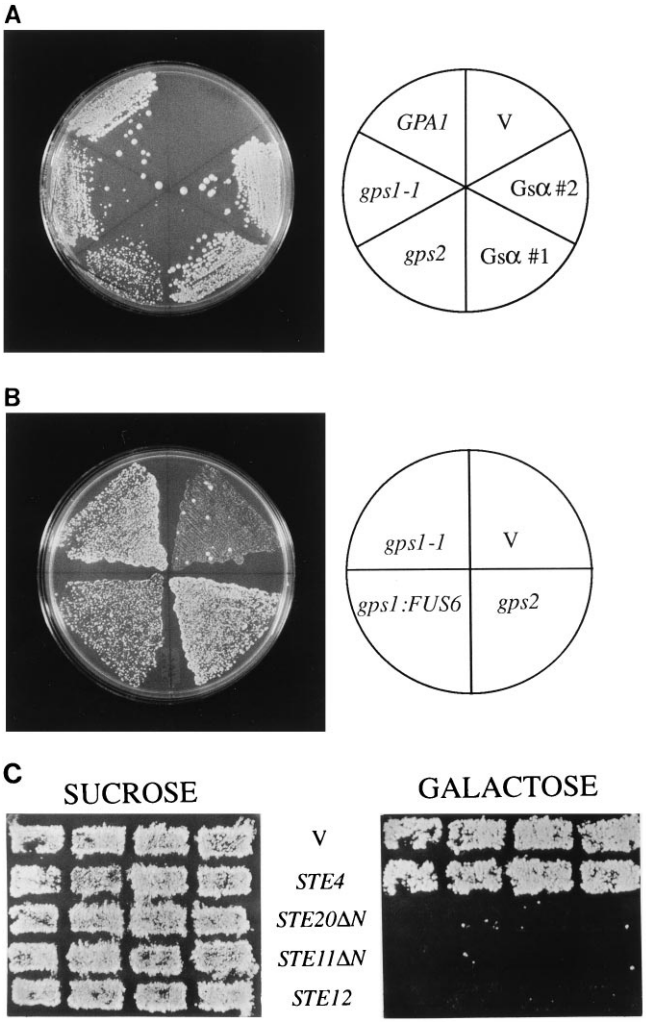

FIG. 1. Assays for suppression of pheromone pathway-activating mutations. (A) Suppression of a *gpa1* mutation. Yeast cells carrying the *gpa1* mutation with a maintenance plasmid (strain LG2TG) were transformed with the indicated constructs and tested for suppressor function by plasmid exchange assay (equal culture volumes were plated). Gsα #1 and #2 represent two of three independently isolated human Gsα clones; *GPA1* represents YEpGPA1; V represents pADNS (empty vector). (B) Pathway activation through a dominant *STE4* mutation. Cells carrying a $STE4^{Hpl}$ mutation and a maintenance plasmid (strain DBC) were transformed with the indicated constructs (V, pADNS; *gps1-1*, p19A; *gps2*, p17B; *gps1*:*FUS6*, pKB251) and subjected to a plasmid exchange assay (equal culture volumes were plated). For cells transformed with vector only, some occasional revertant colonies commonly appear. (C) Pheromone pathway-activating mutations in diploid cells. W303-1A/1B diploid cells were transformed with a plasmid encoding galactose-inducible *STE4* (YCpGAL-STE4), *STE20*Δ*N* (pM4GT-STE20ΔN), *STE11*Δ*N* (pKB254), or *STE12* (pGK40). Quadruplicate patches were replica plated onto sucrose (noninducing) or galactose (inducing) media. The galactose media patches were re-replica plated to eliminate background growth.

TABLE 1. Suppression of *FUS1-lacZ* induction

Suppressor	β-Galactosidase activity with indicated activation gene[a]			
	STE4	*STE20ΔN*	*STE11ΔN*	*STE12*
Vector	1.0	1.0	1.0	1.0
gps1-1	0.8	1.1	0.9	1.0
gps2	0.4	0.7	0.7	0.7
MSG5	0.1	0.1	0.1	0.7
GPA1	0.6	1.0	1.1	0.9

[a] β-Galactosidase activities from cells expressing activation genes were at least 25-fold above values obtained in parallel experiments with vector only. In each column, values were normalized to that for the unsuppressed (activator plus vector) signal, thereby allowing comparison across rows. Each assay was performed at least twice in triplicate with nearly identical results, and the normalized values shown were derived from data with a standard deviation of 10% or less. Constructs used are described in Materials and Methods.

and should therefore block the phosphorylation believed necessary for Ste12p activation (55) and *FUS1* induction. Overexpressed *MSG5* strongly interfered with overexpressed *STE4*-, *STE20ΔN*-, and *STE11ΔN*-mediated signals. In contrast, *MSG5* only moderately reduced (30%) the overexpressed *STE12*-induced *FUS1*::*lacZ* signal. This result is consistent with the observation that overexpressed *STE12* can stimulate *FUS1* in the absence of both *FUS3* and *KSS1* (23). This finding may indicate that some Ste12p phosphorylation is carried out by kinases (other than Fus3p and Kss1p) that are not Msg5p repressible or that unphosphorylated Ste12p is responsible for much of the *FUS1* induction signal, at least in a *STE12*-overexpressing cell (25, 69).

Because the level of interference with *STE4*-induced *FUS1* expression by *gps1-1* is slight and no suppression of downstream inducers was detected, these data do not significantly alter the site-of-action conclusions derived from the lethality suppression results which suggest that *gps1-1* suppression takes place upstream of STE20. *gps2* shows clear suppression of the *STE4* signal (stronger than *GPA1*-mediated suppression), with much less effect on downstream initiators. These results suggest that *gps2* may act primarily upstream of *STE20*, with a reduced (perhaps indirect) effect on downstream signaling elements.

Morphologically distinct suppression by *gps1-1* and *gps2*. In a normal mating response, cell cycle arrest occurs concomitantly with a differentiation program that leads to morphologically altered cells (shmoos) that are enlarged and elongated. These changes are reversed following cell fusion or as a result of adaptation. Cells that carry a lethal, activated G protein appear to expire in this differentiated state (12, 17, 40). Although both *gps1-1* and *gps2* clearly suppress the lethality of a constitutively active pheromone signal (Fig. 1), causing a resumption of vegetative growth, under some conditions they do not equally suppress cellular differentiation. As shown in Fig. 2, cells overexpressing *STE4* and *gps1-1* appear to have morphologies close to normal, whereas many of the cells overexpressing *STE4* and *gps2* are greatly enlarged and elongated. Unlike normal mating shmoos or terminal shmoos resulting from overactivation of the pathway, however, these cells have bypassed cell cycle arrest and are dividing.

***gps1-1* and *gps2* alter cellular response to α-factor.** Haploid yeast cells cultured on solid media produce a zone of growth inhibition, or halo, surrounding a source of pheromone. Eventually, cells may adapt to the pheromone, reenter the cell cycle, and resume vegetative growth, giving rise to colonies within the halo. This adaptation response involves multiple signaling components (reviewed in references 2 and 32).

We examined the α-factor response of **a** cells transformed with *gps1-1* or *gps2*. These cells formed a halo of the same diameter as cells transformed with vector only (Fig. 3). This result suggested that *gps1-1* and *gps2* do not significantly alter the initial firing of the pathway or the sensitivity of cells to pheromone. Although we have demonstrated that *gps2* can reduce the level of *FUS1* induction following overexpression of *STE4* (Table 1), this level of suppression is apparently unable to block the initial arrest response observed in the halo assay. It should be noted that other high-copy-number pheromone pathway suppressors (including *GPA1*) also show a normal halo radius (19, 56). After further incubation, however, a change was noted. As seen in Fig. 3, cells expressing *gps2* have adapted, as indicated by the resumption of growth within the halo region, whereas vector only cells showed no such growth. For *gps1-1*, there was also a resumption of growth, but this was confined primarily to the periphery of the halo. After longer incubation, *gps1-1*-transformed cells also showed some growth throughout the halo. These halo suppression experiments were conducted in wild-type cells and in two pheromone-supersensitive strains. *sst1* mutants are defective in degradation of the α-factor pheromone (35), while *sst2* mutants have a defect in an independent adaptation pathway that is less well understood (18, 51, 62). Expression of *gps1-1* or *gps2* in each of these strains caused halo fill-in, with the *sst2* strain showing more rapid and more extensive halo fill-in than the others (Fig. 3 and data not shown). Therefore, the observed growth within the halos could reflect an enhanced adaptive response that involves neither Sst1p nor Sst2p. Alternatively, it may result from nonadaptive signal attenuation.

When cells were treated with α-factor and examined microscopically, *gps1-1* and *gps2* had no noticeable effect on the rate of cell cycle arrest (nearly 100% unbudded within 3 h [data not shown]), supporting the conclusion that the suppressors do not dramatically block the initial pheromone response. The suppressors also had no effect on the initial rate of reentry into the cell cycle following pheromone withdrawal, indicating that *gps1-1* and *gps2* do not dramatically affect recovery following transient pheromone exposure. These conditions are distinct, however, from the long-term chronic pheromone exposure in the halo assay and the crisis situation arising from a mutation causing constitutive pathway activation.

***gps1* is structurally and functionally related to *Arabidopsis FUS6* (*COP11*).** Northern analysis indicated that both *gps1* and *gps2* are expressed in a wide variety of human tissues (Fig. 4). In both cases, one principal transcript was evident. For *gps1*, an additional low-abundance species of larger size was also detectable. The sizes of the major mRNA species indicated that the *gps1-1* isolate was truncated and that the *gps2* isolate was near full length in size. Through cDNA library screening and primer extension, full-length clones were obtained.

Sequence analysis of full-length *gps1* indicated that the predicted protein sequence is longer at its amino terminus than the original *gps1-1* isolate (Fig. 5). Two possible initiation sites are separated by 13 codons, and both are in regions that conform well to translation start consensus sequences (31). Yeast expression clones were engineered to initiate at each of these possible start sites, and an amino-terminal epitope tag was incorporated into these constructs as well as the original suppressing clone. Western blot analysis indicated that both of the larger constructs yielded products of the expected size (with some apparent breakdown products) and were expressed at levels comparable to that of the original truncated suppressor form of *gps1* (data not shown). Although the epitope-tagged *gps1-1* construct retained suppressor activity, the putative full-length constructs suppressed neither the *gpa1* mutation (data

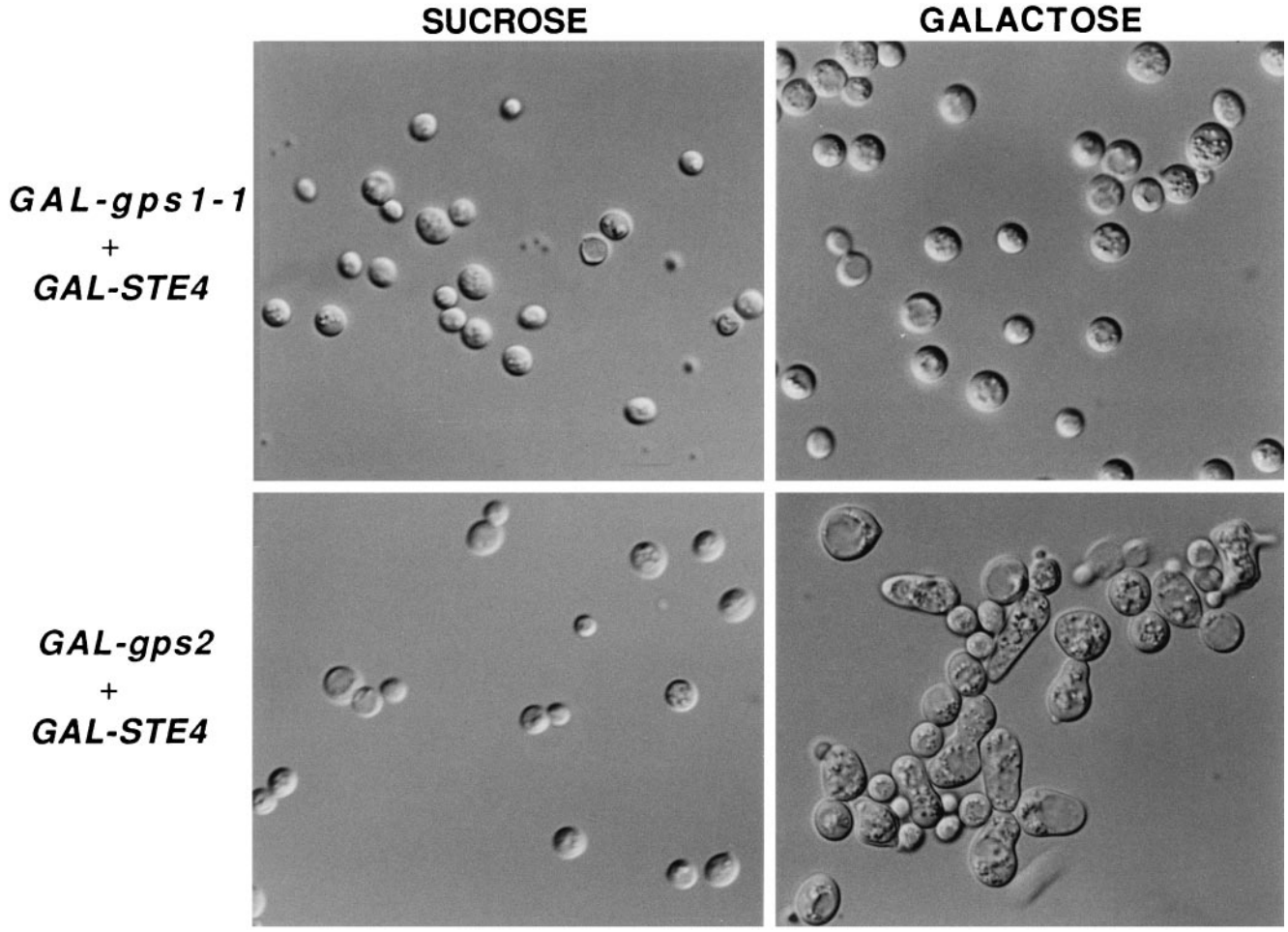

FIG. 2. Suppression of pathway-induced cell morphology changes. Wild-type cells (W303-1A) were transformed with galactose-inducible constructs of *STE4* (YCpGAL-STE4) and either *gps1-1* (pKB247) or *gps2* (pKB241). These cells were then grown under noninducing (sucrose; left) or inducing (galactose; right) conditions. Induced cells with pKB247 and pKB241 alone had normal morphologies (data not shown). Photos were taken by using a Nikon FXA microscope with a 60× objective and differential interference contrast (Nomarski) optics.

not shown) nor the $STE4^{Hpl}$ mutation (Fig. 6). The additional amino-terminal sequences of *gps1*, then, appear to have reduced or eliminated suppressor function in yeast. To further define the primary sequence requirements for G-protein pathway suppression, deletion mutations of *gps1-1* were created and analyzed. As shown in Fig. 6, carboxy-terminal and internal deletions of Gps1-1 abolished suppressor activity.

Examination of the Gps1 sequence revealed extensive similarity to the predicted protein encoded by the *Arabidopsis FUS6* (*COP11*) gene (8). *FUS6* appears to be expressed in all plant tissues and is essential for plant development: some *fus6* mutants are so severely disrupted that they rarely develop beyond the seedling stage (8). Mutations in this gene also cause a constitutive photomorphogenesis phenotype (61), suggesting that the function of *FUS6* is to negatively regulate a light-mediated signaling pathway. As shown in Fig. 5, Gps1 and FUS6 have 47% identity and 64% similarity. The alignment covers almost the entire sequence of FUS6 and requires few gaps. This finding suggested that these evolutionarily distant gene products may also be functionally related. Although *FUS6* sequences alone did not provide detectable suppression of the $STE4^{Hpl}$ mutation, even when truncated to approximate the *gps1-1* clone, a chimeric *gps1*:*FUS6* construct showed activity that was only slightly reduced from the original *gps1-1* clone (Fig. 1B). As shown in Fig. 6, the chimera was made by replacing an essential region of Gps1-1 with corresponding FUS6 sequences. These results demonstrated that human *gps1* and *Arabidopsis FUS6* are indeed functionally related.

The sequence of Gps2 (Fig. 7) revealed no significant similarity to known proteins, and it contains no consensus patterns or motifs indicative of function. The original library isolate of *gps2* appears to contain the entire coding sequence of this gene, although primer extension revealed a short addition to the upstream noncoding region. Constructs in which the library

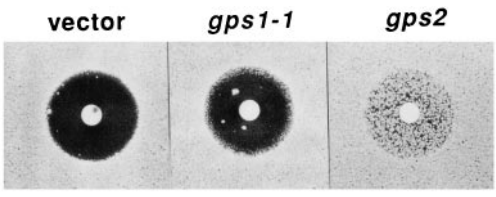

FIG. 3. Halo assay of pheromone response. *sst1* cells (GPY74-15Ca), transformed with the indicated construct (vector [pADANS], *gps1-1* [p19A], or *gps2* [p17B]), were exposed to an α-factor-soaked filter. Cells were grown for 6 days before photography, although growth within the halos was apparent within 3 days.

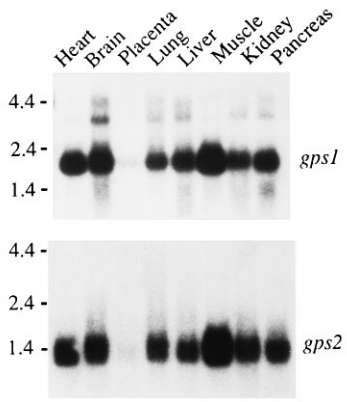

FIG. 4. Northern analysis of *gps1* and *gps2* expression in human tissue. Multiple Tissue Northern blots (Clontech) were probed with *gps1* (top) or *gps2* (bottom). Subsequent probing with actin verified approximately equal RNA loading except for reduced levels in placenta (data not shown). Markers (kilobases) are given at left.

vector Adh1 fusion sequence was replaced with an epitope tag retained suppressor function, indicating that the fusion sequences were not involved.

***gps1* and *gps2* act as signal suppressors in mammalian cells.** The ability of *gps1* and *gps2* to interfere with RAS- and MAP kinase-mediated signaling in mammalian cells was first tested in a reporter gene induction assay. The *PGS2* promoter-driven luciferase reporter has been shown to respond to signals initiated by an activated *src* allele (66). This induction is strongly inhibited by dominant negative forms of RAS, ERK, and JNK, demonstrating that it relies on both the ERK and JNK MAP kinase cascades (67). As shown in Fig. 8, NIH 3T3 cells cotransfected with the *PGS2*-luciferase reporter and v-*src* activator showed strong induction (31-fold). This transcriptional activation was blocked, as expected, by a dominant negative H-*ras* allele. *gps1* and *gps2* also showed potent repression of the transcriptional activation signal (six- and fourfold, respectively), and the level of repression was dependent on the amount of *gps1* or *gps2* DNA used. Expression of *gps1-1*, the truncated version of *gps1*, was also able to suppress the inductive signal, although not as strongly as full-length *gps1* (data not shown). This result is in contrast to the signal suppression results in yeast, where *gps1-1* behaved as a potent suppressor but full-length *gps1* had no detectable suppression activity (Fig. 6). This finding may indicate that the amino-terminal portion of *gps1* mediates a function (e.g., effector binding) that strengthens signal repression in mammalian cells but is antagonistic to signal repression in yeast.

To more directly determine the effects of *gps1* and *gps2* on signal transduction, we measured the activity of JNK1, the terminal kinase of a MAP kinase cascade that can be activated by RAS. JNK1 activity is stimulated by a variety of extracellular stimuli and is present in cultured cells grown in the presence of serum (28). Catalytically active JNK1 phosphorylates the transcription factor JUN. Using an immunocomplex JNK1 kinase assay, we observed that transfected *gps1* and *gps2* reduced JNK1 activity 3- and 18-fold, respectively (Fig. 9). Dominant negative RAS produced a fivefold reduction in JNK1 activity. When the JNK1 signal was enhanced by cotransfection with v-*src*, suppression was still observed (data not shown). Therefore, overexpressed *gps1* and *gps2* can suppress G protein (RAS)- and MAP kinase-mediated signaling in mammalian cells and, more specifically, interfere with JNK1 activity. Taken together with the observed effects in yeast cells, these data suggest that *gps1* and *gps2* normally function as signal attenuators.

DISCUSSION

Yeast signal transduction pathway mutants have proven to be powerful tools for the isolation and characterization of signaling components from higher eukaryotes (3, 14). The suppression of a yeast G-protein–MAP kinase pathway by human *gps1-1* and *gps2*, as well as the *gps1*:*FUS6* chimera, provides further evidence that signaling effectors and regulators are evolutionarily conserved. These suppressors likely act on pheromone pathway components common to both **a** and α cells, since they suppress a *gpa1* mutation in both cell types. *gps1-1* and *gps2* differ, however, in their relative abilities to block differentiation and promote recovery. In cells overexpressing Ste4p, both can relieve cell cycle arrest and permit cell division, but *gps2*-expressing cells retain morphological features of differentiated cells. This could reflect a difference in the magnitude of suppression. However, when pheromone response was examined by halo and *FUS1* induction assays, *gps2* gave rise to more extensive interference than did *gps1-1*. These observed

```
Gps1  MEVDGTPRRGGCKMPLPVQVFNLQGAVEPMQIDVDPQEDPQNAPDVNYVVENPSLDLEQYAASYSGLMRIERQLFIADHCP...TLRVEALKMALS   93
FUS6                    MERDEEAGGPMMEMCTNGGEETSNRRP...IISGEPLDIEAYAALYKGRTKIMRLLFIANHCGGNHALQFDALRMAYD   75

FVQRTFNVDMYEEIHRKLSEATRELQNAPDAIPESGVEPPALDTAWVEATRKKALLKLEKLDTDLKNYKGNSIKESIRRGHDDLGDHYLDCGDLSNALKCYS  195
EIKKGENTQLFREVVNK.............IGNRLGEKYGMDLAWCEAVDRRAEQKKVKLENELSSYRTNLIKESIRMGYNDFGDFYYACGMLGDAFKNYI  163

                                          *
RARDYCTSAKHVINMCLNVIKVSVYLQNWSHVLSYVSKAESTPEIAEQRGERDSQTQAILTKLKCAAGLAELAARKYKQAAKCLLLASFDHCD.FPELLSPS  296
RTRDYCTTTKHIIHMCMNAILVSIEMGQFTHVTSYVNKAEQNPETLEPM.........VNAKLRCASGLAHLELKKTKLAARKFLDVNPELGNSYNEVIAPQ  256

NVAIYGGLCALATFDRQELQRNVISSSSFKLFLELEPQVRDIIFKFYESKYASCLKMLDEMKDNLLLDMYLAPHVRTLYTQIRNRALIQYFSPYVSADMHRM  398
DIATYGGLCALASFDRSELKQKVIDNINFRNFLELVPDVRELINDFYSSRYASCLEYLASLKSNLLLDIHLHDHVDTLYDQIRKKALIQYTLPFVSVDLSRM  358

AAAFNTTVAALEDELTQLILEGLISARVDSHSKILYARDVDQRSTTFEKSLLMGKEFQRRAKAMMLRAAVLRNQIHVKSPPREGSQGELTPANSQSRMSTNM  500
ADAFKTSVSGLEKELEALITDNQIQARIDSHNKILYARHADQRNATFQKVLQMGNEFDRDVRAMLLRANLLKHEYHARSARKL                      441
```

FIG. 5. Predicted amino acid sequence of Gps1 and alignment with FUS6. The start position of Gps1-1, following the Adh1 or HA epitope fusion peptide, is indicated with an asterisk. Gps1 and FUS6 were aligned by using the BLAST algorithm (1). Lines, double dots, and single dots represent identity, strong conservation, and weak conservation, respectively. The region of Gps1 sequence replaced with FUS6 sequence in the Gps1:FUS6 chimera (Fig. 7) is underlined. GenBank accession numbers: U20285 (Gps1) and L26498 (FUS6).

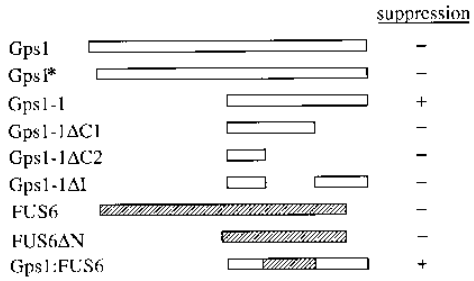

FIG. 6. *STE4*^{Hpl} suppression capability of *gps1* and *FUS6* constructs. The predicted Gps1 protein products (open boxes) and FUS6 protein products (hatched boxes) and a chimeric protein product are shown approximately to scale and aligned. Gps1* represents the product from a construct designed to initiate at the second in-frame ATG. Note that all constructs are expressed as either Adh1 or HA epitope peptide fusions.

differences may indicate that *gps1-1* and *gps2* act through distinct mechanisms.

That *gps1-1* and *gps2* block lethality resulting from overexpressed Ste4p or dominant active mutant Ste4p (Ste4^{Hpl}p) is consistent with their acting at or downstream of this point in the pathway. If they suppressed at the level of the G protein itself, however, they would have to be unaffected by the *STE4*^{Hpl} mutation, which blocks the interaction between Ste4p and its negative regulator Gpa1p (Gα). Downstream suppression could occur through activation of an adaptation program that overrides the unremitting signal (although Sst1p and Sst2p do not seem to be involved). This possibility is consistent with the observations that *gps1-1*- and *gps2*-expressing cells display an initial pheromone response that appears normal (as judged by halo assay and the microscopic analysis of cells treated with pheromone). Although the initial recovery of cells following short-term exposure to pheromone was also unaffected, both *gps1-1* and *gps2* enhanced recovery from chronic exposure to pheromone in the halo assay, and each suppressed the lethality of G-protein mutations leading to pathway activation. These results highlight the distinction between transient signaling and the crisis situation resulting from constitutive signaling. Suppression by *gps1-1* and *gps2* might be mediated by enhancement of an adaptation pathway which can overcome a chronic signal. Alternatively, these suppressors may work through inhibition of a signaling component that is not normally a target of the adaptation pathways. In this case, the level of inhibition might be insufficient to prevent the physiological response from the initial signal but enough to avert the lethal consequences of prolonged signal transduction.

Recovery from chronic signaling could occur at many levels, including an increase in G_1 cyclin-dependent kinase activity (i.e., relieving repression of G_1 cyclin[s]). Fus3p, one of the pheromone-induced MAP kinases, phosphorylates and activates Far1p (46, 59), which is a repressor of the Cdc28p cyclin-dependent kinase (47). Interestingly, both *FUS3* (24) and *FAR1* (10) were identified through recessive mutants that were defective in establishing pheromone-induced cell cycle arrest but showed near-normal control of *FUS1* induction. Additionally, *far1* and *fus3* mutants have the appearance of differentiated cells following pathway activation. The somewhat differentiated morphology of *STE4*-overexpressing cells expressing *gps2* may indicate a direct or indirect impact on G_1 cyclin control.

The inability of *gps1-1* and *gps2* to suppress the lethality of *STE20*Δ*N*, *STE11*Δ*N*, and overexpressed *STE12* was perhaps not surprising. Ste20p participates in multiple pathways (16), and cell death caused by mutant *STE20* is known to involve a

```
MPALLERPKLSNAMARALHRHIMMERERKRQEEEEVDKMMEQKMKEEQERRKKKE   55
MEERMSLEETKEQILKLEEKLLALQEEKEQLFLQLKKVLHEEEKRRRKEQSDLTT  110
LTSAAYQQSLTVHTGTHLLSMQGSPGGHNRPGTLMAADRAKQMFGPQVLTTRHYV  165
GSAAAFAGTPEHGQFQGSPGGAYGTAQPFPHYGPTQPAYSPSQQLRAPSAFPAVQ  220
YLSQPQPQPYAVHGHFQPTQTGFLQPGGALSLQKQMEHANQQTGFSDSSSLRPMH  275
PQALHPAPGLLASPQLPVQMQPAGKSGFNATSQPGPRLPFIQHSQNPRFYHK     327
```

FIG. 7. Predicted amino acid sequence of Gps2. GenBank accession number: U28963.

non-pheromone pathway component (reference 50 and this work) which is apparently unaffected by these suppressors. Our data suggest that *STE11*Δ*N*-induced lethality also involves factors outside the pheromone response pathway. It should be noted that Ste20p, Ste11p, and Ste12p have all been implicated in the pseudohyphal growth induction pathway (52), and this additional signaling capacity may contribute to their lethal phenotypes when constitutively activated.

Signal repression could involve direct effects on transcription, thereby leading to a change in the expression level(s) of a key signaling component(s). This might overcome the lethality of constitutive signaling without grossly altering the initial pheromone response. However, such a mechanism could not require induction of *GPA1*, since *gps1-1* and *gps2* suppress a *gpa1* mutant. Neither could it require repression of *STE4*, since they suppress a *GAL1* promoter-driven *STE4* construct. Other genes involved in signal transduction, adaptation, or cell cycle control could be the targets of such transcriptional control. In the case of *gps2*, there was also a moderate reduction in the level of *FUS1* induction by *STE20*Δ*N*, *STE11*Δ*N*, and *STE12*.

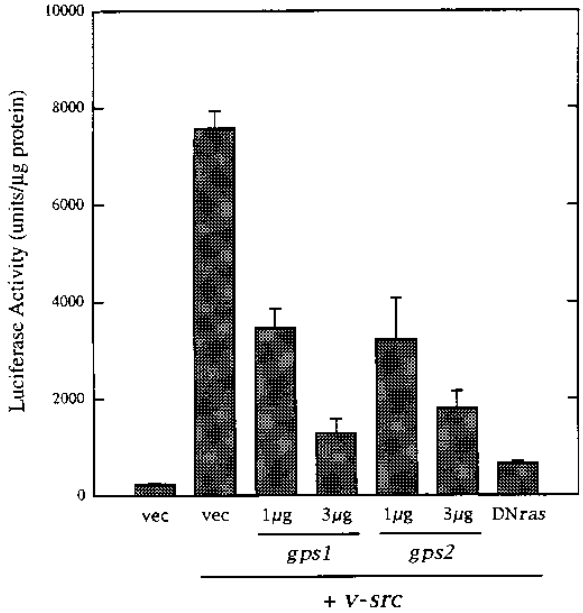

FIG. 8. Effects of *gps1* and *gps2* on reporter gene induction in mammalian cells. NIH 3T3 cells were transiently transfected with a *PGS2*-luciferase reporter construct, with a v-*src* construct or equivalent vector, and with the test expression construct (*gps1* or *gps2*) or empty expression vector (vec). *gps1* and *gps2* were expressed from a pcDNA3 vector that was modified to include an HA epitope tag. This modified plasmid, pcDNA3-HA, was used as the control vector. The amount of suppression plasmid used is indicated. Three micrograms of dominant negative *ras* (DN*ras*) plasmid DNA was used. The suppression data shown represent the mean values of three independent experimental points. In a separate experiment, similar results were obtained.

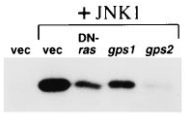

FIG. 9. *gps1* and *gps2* repress JNK1 activity. NIH 3T3 cells were transfected with 9 μg of vector (pcDNA3-HA), dominant negative *ras* (DN-*ras*) (pZIPN17), *gps1* (pcDNA3-HAGPS1), or *gps2* (pcDNA3-HAGPS2) along with either 4 μg of JNK1 (pcDNA-FlagJNK1) or 4 μg of vector as indicated. The immunocomplex kinase assay using a GST–c-Jun substrate was performed as described in Materials and Methods. Two additional independent experiments produced similar results. The fold repression mean values (compared to Flag-JNK1 plus vector) for the three experiments were 7.2-fold for DN-*ras* 4.4-fold for *gps1*, and 18-fold for *gps2*.

Although this finding raises the possibility that Gps2 directly represses Ste12p activity, no suppression of *STE12* overexpression lethality was observed. Furthermore, overexpressed *STE12* has been shown to retain much of its *FUS1* activation potential even under conditions where it is unlikely to be phosphorylated (reference 23 and this work). The moderate effects of *gps2* on the overexpressed *STE12* signal, therefore, may be the result of an indirect mechanism.

Analysis of *gps1* indicates that its relationship to the *Arabidopsis FUS6* (*COP11*) gene goes well beyond extensive primary sequence conservation and broad tissue-type expression patterns. We have shown that a highly conserved portion of *FUS6* (*COP11*) can functionally substitute for an equivalent region of *gps1-1* that is required for suppression of G-protein signaling. It is not yet clear, however, whether this reflects a conserved enzymatic activity, a capacity to bind a critical signaling component, or a structural feature essential for one of these functions. The signal transduction interference properties of both *gps1-1* and the *gps1*:*FUS6* chimera are consistent with the proposed repressor function of *FUS6* (*COP11*) in light-mediated signaling (9; reviewed in reference 5). In the yeast assay, the carboxy-terminal half of Gps1 is sufficient for signal suppression but replacement of its amino-terminal residues abolishes suppressor activity, raising the possibility that a form of dominant interference is involved. In mammalian cells, however, full-length *gps1* is the more potent signal suppressor, suggesting that in this native cell context, full suppressor function may involve both protein domains. While there is no evidence that *S. cerevisiae* encodes true homologs of Gps1 or Gps2, our data indicate that these proteins affect closely related pathways from yeast to mammalian cells, suggesting that they are capable of functionally interacting with conserved signal transduction proteins.

The experiments described here further demonstrate that simple eukaryotes can be used to identify human signal transduction components, including signal repressors, and to probe their functions. Although the phenotypic endpoints of the RAS, heterotrimeric G-protein, and MAP kinase pathways differ between these organisms, recent work has revealed a remarkable conservation of structure, function, and regulation of many components (21, 29, 38, 45, 49, 54). The finding that overexpressed *gps1* or *gps2* results in suppression of a small G-protein (RAS)- and MAP kinase-mediated signal in mammalian cells (in both reporter gene and kinase assays) lends strong support to the model that these proteins normally function as signal repressors. The possibility that *gps1* and *gps2* act as dedicated inhibitors or repressors of conserved signaling pathways suggests a level of regulation that deserves further examination. In addition, *gps1* is itself a highly conserved gene, and examination of its function may further elucidate the role of *FUS6* (*COP11*) in plant development.

ACKNOWLEDGMENTS

K. Bowdish and B. Spain contributed equally to this work.

We thank K.-T. Jeang and D.-Y. Jin for providing a sequence correction of *gps2*; R. Rothstein, R. Kornberg, S. I. Reed, S. Fields, J. Thorner, I. Herskowitz, J. J. Harada, M. A. L. West, G. Cooper, R. Davis, and H. R. Herschman for providing essential strains and plasmids, and K. Elwood, B. Dzudzor, and L. Han for technical assistance. K.-T. Jeang, H. R. Herschman, S. Fields, J. Thorner, and L. Bardwell were also involved in critical discussions during the preparation of the manuscript.

This work was supported by Department of Energy contract DE FC03 87ER60615, National Institutes of Health grants CA 56301 and GM 24787 (to H. R. Herschman for W. Xie), and the Jonsson Cancer Center Foundation.

REFERENCES

1. **Altschul, S. F., W. Gish, W. Miller, E. W. Myers, and D. J. Lipman.** 1990. Basic local alignment search tool. J. Mol. Biol. **215:**403–410.
2. **Bardwell, L., J. G. Cook, C. J. Inouye, and J. Thorner.** 1994. Signal propagation and regulation in the mating pheromone response pathway of the yeast Saccharomyces cerevisiae. Dev. Biol. **166:**363–379.
3. **Bender, J., and G. R. Fink.** 1994. AFC1, a LAMMER kinase from Arabidopsis thaliana, activates STE12-dependent processes in yeast. Proc. Natl. Acad. Sci. USA **91:**12105–12109.
4. **Blinder, D., S. Bouvier, and D. D. Jenness.** 1989. Constitutive mutants in the yeast pheromone response: ordered function of the gene products. Cell **56:**479–486.
5. **Bowler, C., and N. H. Chua.** 1994. Emerging themes of plant signal transduction. Plant Cell **6:**1529–1541.
6. **Cai, H., J. Szeberenyi, and G. M. Cooper.** 1994. Effect of a dominant inhibitory Ha-*ras* mutation on mitogenic signal transduction in NIH 3T3 cells. Mol. Cell. Biol. **10:**5314–5323.
7. **Cairns, B. R., S. W. Ramer, and R. D. Kornberg.** 1992. Order of action of components in the yeast pheromone response pathway revealed with a dominant allele of the STE11 kinase and the multiple phosphorylation of the STE7 kinase. Genes Dev. **6:**1305–1318.
8. **Castle, L. A., and D. W. Meinke.** 1994. A FUSCA gene of Arabidopsis encodes a novel protein essential for plant development. Plant Cell **6:**25–41.
9. **Chamovitz, D. A., W. Ning, M. T. Osterlund, A. G. von Arnim, J. M. Staub, M. Matsui, and X.-W. Deng.** The COP9 complex, a novel multisubunit nuclear regulator involved in light control of a plant developmental switch. Cell **86:**115–121.
10. **Chang, F., and I. Herskowitz.** 1990. Identification of a gene necessary for cell cycle arrest by a negative growth factor of yeast: FAR1 is an inhibitor of a G1 cyclin, CLN2. Cell **63:**999–1011.
11. **Choi, K. Y., B. Satterberg, D. M. Lyons, and E. A. Elion.** 1994. Ste5 tethers multiple protein kinases in the MAP kinase cascade required for mating in S. cerevisiae. Cell **78:**499–512.
12. **Cole, G. M., D. E. Stone, and S. I. Reed.** 1990. Stoichiometry of G protein subunits affects the *Saccharomyces cerevisiae* mating pheromone signal transduction pathway. Mol. Cell. Biol. **10:**510–517.
13. **Colicelli, J., C. Birchmeier, T. Michaeli, K. O'Neill, M. Riggs, and M. Wigler.** 1989. Isolation and characterization of a mammalian gene encoding a high-affinity cAMP phosphodiesterase. Proc. Natl. Acad. Sci. USA **86:**3599–3603.
14. **Colicelli, J., C. Nicolette, C. Birchmeier, L. Rodgers, M. Riggs, and M. Wigler.** 1991. Expression of three mammalian cDNAs that interfere with RAS function in *Saccharomyces cerevisiae*. Proc. Natl. Acad. Sci. USA **88:** 2913–2917.
15. **Crespo, P., T. G. Cachero, N. Xu, and J. S. Gutkind.** 1995. Dual effect of beta-adrenergic receptors on mitogen-activated protein kinase. Evidence for a beta gamma-dependent activation and a G alpha s-cAMP-mediated inhibition. J. Biol. Chem. **270:**25259–25265.
16. **Cvrckova, F., C. De Virgilio, E. Manser, J. R. Pringle, and K. Nasmyth.** 1995. Ste20-like protein kinases are required for normal localization of cell growth and for cytokinesis in budding yeast. Genes Dev. **9:**1817–1830.
17. **Dietzel, C., and J. Kurjan.** 1987. The yeast *SCG1* gene: a G-alpha-like protein implicated in the a- and alpha-factor response pathway. Cell **50:** 1001–1010.
18. **Dietzel, C., and J. Kurjan.** 1987. Pheromonal regulation and sequence of the *Saccharomyces cerevisiae SST2* gene: a model for desensitization to pheromone. Mol. Cell. Biol. **7:**4169–4177.
19. **Doi, K., A. Gartner, G. Ammerer, B. Errede, H. Shinkawa, K. Sugimoto, and K. Matsumoto.** 1994. MSG5, a novel protein phosphatase promotes adaptation to pheromone response in S. cerevisiae. EMBO J. **13:**61–70.
20. **Dolan, J. W., and S. Fields.** 1990. Overproduction of the yeast STE12 protein leads to constitutive transcriptional induction. Genes Dev. **4:**492–502.
21. **Druey, K. M., K. J. Blumer, V. H. Kang, and J. H. Kehrl.** 1996. Inhibition of G-protein-mediated MAP kinase activation by a new mammalian gene family. Nature (London) **379:**742–746.

22. **Elion, E. A.** 1995. Ste5: a meeting place for MAP kinases and their associates. Trends Cell Biol. **5:**322–327.
23. **Elion, E. A., J. A. Brill, and G. R. Fink.** 1991. FUS3 represses CLN1 and CLN2 and in concert with KSS1 promotes signal transduction. Proc. Natl. Acad. Sci. USA **88:**9392–9396.
24. **Elion, E. A., P. L. Grisafi, and G. R. Fink.** 1990. FUS3 encodes a cdc2+/CDC28-related kinase required for the transition from mitosis into conjugation. Cell **60:**649–664.
25. **Errede, B., and G. Ammerer.** 1989. STE12, a protein involved in cell-type-specific transcription and signal transduction in yeast, is part of protein-DNA complexes. Genes Dev. **3:**1349–1361.
26. **Faure, M., T. A. Voyno-Yasenetskaya, and H. R. Bourne.** 1994. cAMP and beta gamma subunits of heterotrimeric G proteins stimulate the mitogen-activated protein kinase pathway in COS-7 cells. J. Biol. Chem. **269:**7851–7854.
27. **Herskowitz, I.** 1995. MAP kinase pathways in yeast: for mating and more. Cell **80:**187–197.
28. **Hibi, M., A. Lin, T. Smeal, A. Minden, and M. Karin.** 1993. Identification of an oncoprotein- and UV-responsive protein kinase that binds and potentiates the c-Jun activation domain. Genes Dev. **7:**2135–2148.
29. **Hill, C. S., J. Wynne, and R. Treisman.** 1995. The Rho family GTPases RhoA, Rac1, and CDC42Hs regulate transcriptional activation by SRF. Cell **81:**1159–1170.
30. **Johnston, M., and R. W. Davis.** 1984. Sequences that regulate the divergent *GAL1-GAL10* promoter in *Saccharomyces cerevisiae*. Mol. Cell. Biol. **4:**1440–1448.
31. **Kozak, M.** 1987. An analysis of 5′-noncoding sequences from 699 vertebrate messenger RNAs. Nucleic Acids Res. **15:**8125–8148.
32. **Kurjan, J.** 1993. The pheromone response pathway in Saccharomyces cerevisiae. Annu. Rev. Genet. **27:**147–179.
33. **Leberer, E., D. Dignard, D. Harcus, D. Y. Thomas, and M. Whiteway.** 1992. The protein kinase homologue Ste20p is required to link the yeast pheromone response G-protein beta gamma subunits to downstream signalling components. EMBO J. **11:**4815–4824.
34. **Levin, D. E., and B. Errede.** 1995. The proliferation of MAP kinase signaling pathways in yeast. Curr. Opin. Cell Biol. **7:**197–202.
35. **MacKay, V. L., S. K. Welch, M. Y. Insley, T. R. Manney, J. Holly, G. C. Saari, and M. L. Parker.** 1988. The Saccharomyces cerevisiae BAR1 gene encodes an exported protein with homology to pepsin. Proc. Natl. Acad. Sci. USA **85:**55–59.
36. **Manser, E., T. Leung, H. Salihuddin, Z. S. Zhao, and L. Lim.** 1994. A brain serine/threonine protein kinase activated by Cdc42 and Rac1. Nature (London) **367:**40–46.
37. **Marcus, S., A. Polverino, E. Chang, D. Robbins, M. H. Cobb, and M. H. Wigler.** 1995. Shk1, a homolog of the Saccharomyces cerevisiae Ste20 and mammalian p65PAK protein kinases, is a component of a Ras/Cdc42 signaling module in the fission yeast Schizosaccharomyces pombe. Proc. Natl. Acad. Sci. USA **92:**6180–6184.
38. **Mattingly, R. R., and I. G. Macara.** 1996. Phosphorylation-dependent activation of the Ras-GRF/CDC25Mm exchange factor by muscarinic receptors and G-protein subunits. Nature (London) **382:**268–272.
39. **Minden, A., A. Lin, M. McMahon, C. Lange-Carter, B. Derijard, R. J. Davis, G. L. Johnson, and M. Karin.** 1994. Differential activation of ERK and JNK mitogen-activated protein kinases by Raf-1 and MEKK. Science **266:**1719–1723.
40. **Miyajima, I., M. Nakafuku, N. Nakayama, C. Brenner, A. Miyajima, K. Kaibuchi, K. Arai, Y. Kaziro, and K. Matsumoto.** 1987. *GPA1*, a haploid-specific essential gene, encodes a yeast homolog of mammalian G protein which may be involved in mating factor signal transduction. Cell **50:**1011–1019.
41. **Neer, E. J.** 1995. Heterotrimeric G proteins: organizers of transmembrane signals. Cell **80:**249–257.
42. **Nikawa, J., P. Sass, and M. Wigler.** 1987. Cloning and characterization of the low-affinity cyclic AMP phosphodiesterase gene of *Saccharomyces cerevisiae*. Mol. Cell. Biol. **7:**3629–3636.
43. **Niman, H. L., R. A. Houghten, L. E. Walker, R. A. Reisfeld, I. A. Wilson, J. M. Hogle, and R. A. Lerner.** 1983. Generation of protein-reactive antibodies by short peptides is an event of high frequency: implications for the structural basis of immune recognition. Proc. Natl. Acad. Sci. USA **80:**4949–4953.
44. **Oehlen, B., and F. R. Cross.** 1994. Signal transduction in the budding yeast Saccharomyces cerevisiae. Curr. Opin. Cell Biol. **6:**836–841.
45. **Olson, M. F., A. Ashworth, and A. Hall.** 1995. An essential role for Rho, Rac, and Cdc42 GTPases in cell cycle progression through G1. Science **269:**1270–1272.
46. **Peter, M., A. Gartner, J. Horecka, G. Ammerer, and I. Herskowitz.** 1993. FAR1 links the signal transduction pathway to the cell cycle machinery in yeast. Cell **73:**747–760.
47. **Peter, M., and I. Herskowitz.** 1994. Direct inhibition of the yeast cyclin-dependent kinase Cdc28-Cln by Far1. Science **265:**1228–1231.
48. **Pillai, R., K. Kytle, A. Reyes, and J. Colicelli.** 1993. Use of a yeast expression system for the isolation and analysis of drug-resistant mutants of a mammalian phosphodiesterase. Proc. Natl. Acad. Sci. USA **90:**11970–11974.
49. **Polverino, A., J. Frost, P. Yang, M. Hutchison, A. M. Neiman, M. H. Cobb, and S. Marcus.** 1995. Activation of mitogen-activated protein kinase cascades by p21-activated protein kinases in cell-free extracts of Xenopus oocytes. J. Biol. Chem. **270:**26067–26070.
50. **Ramer, S. W., and R. W. Davis.** 1993. A dominant truncation allele identifies a gene, STE20, that encodes a putative protein kinase necessary for mating in Saccharomyces cerevisiae. Proc. Natl. Acad. Sci. USA **90:**452–456.
51. **Reneke, J. E., K. J. Blumer, W. E. Courchesne, and J. Thorner.** 1988. The carboxy-terminal segment of the yeast alpha-factor receptor is a regulatory domain. Cell **55:**221–234.
52. **Roberts, R. L., and G. R. Fink.** 1994. Elements of a single MAP kinase cascade in Saccharomyces cerevisiae mediate two developmental programs in the same cell type: mating and invasive growth. Genes Dev. **8:**2974–2985.
53. **Schultz, J., B. Ferguson, and G. F. Sprague, Jr.** 1995. Signal transduction and growth control in yeast. Curr. Opin. Genet. Dev. **5:**31–37.
54. **Simon, M. N., C. De Virgilio, B. Souza, J. R. Pringle, A. Abo, and S. I. Reed.** 1995. Role for the Rho-family GTPase Cdc42 in yeast mating-pheromone signal pathway. Nature (London) **376:**702–705.
55. **Song, D., J. W. Dolan, Y. L. Yuan, and S. Fields.** 1991. Pheromone-dependent phosphorylation of the yeast STE12 protein correlates with transcriptional activation. Genes Dev. **5:**741–750.
56. **Spain, B. H., D. Koo, M. Ramakrishnan, B. Dzudzor, and J. Colicelli.** 1995. Truncated forms of a novel yeast protein suppress the lethality of a G protein α subunit deficiency by interacting with the β subunit. J. Biol. Chem. **270:**25435–25444.
57. **Stevenson, B. J., N. Rhodes, B. Errede, and G. F. Sprague, Jr.** 1992. Constitutive mutants of the protein kinase STE11 activate the yeast pheromone response pathway in the absence of the G protein. Genes Dev. **6:**1293–1304.
58. **Tan, P. K., N. G. Davis, G. F. Sprague, Jr., and G. S. Payne.** 1993. Clathrin facilitates the internalization of seven transmembrane segment receptors for mating pheromones in yeast. J. Cell Biol. **123:**1707–1716.
59. **Tyers, M., and B. Futcher.** 1993. Far1 and Fus3 link the mating pheromone signal transduction pathway to three G_1-phase Cdc28 kinase complexes. Mol. Cell. Biol. **13:**5659–5669.
60. **van Biesen, T., B. E. Hawes, D. K. Luttrell, K. M. Krueger, K. Touhara, E. Porfiri, M. Sakaue, L. M. Luttrell, and R. J. Lefkowitz.** 1995. Receptor-tyrosine-kinase- and G beta gamma-mediated MAP kinase activation by a common signalling pathway. Nature (London) **376:**781–784.
61. **Wei, N., S. F. Kwok, A. G. von Arnim, A. Lee, T. W. McNellis, B. Piekos, and X. W. Deng.** 1994. Arabidopsis COP8, COP10, and COP11 genes are involved in repression of photomorphogenic development in darkness. Plant Cell **6:**629–643.
62. **Weiner, J. L., C. Guttierez-Steil, and K. J. Blumer.** 1993. Disruption of receptor-G protein coupling in yeast promotes the function of an SST2-dependent adaptation pathway. J. Biol. Chem. **268:**8070–8077.
63. **West, M. A. L., and J. J. Harada.** Unpublished results.
64. **Whiteway, M., K. L. Clark, E. Leberer, D. Dignard, and D. Y. Thomas.** 1994. Genetic identification of residues involved in association of alpha and beta G-protein subunits. Mol. Cell. Biol. **14:**3223–3229.
65. **Whiteway, M. S., C. Wu, T. Leeuw, K. Clark, A. Fourest-Lieuvin, D. Y. Thomas, and E. Leberer.** 1995. Association of the yeast pheromone response G protein $\beta\gamma$ subunits with the MAP kinase scaffold Ste5p. Science **269:**1572–1575.
66. **Xie, W., B. S. Fletcher, R. D. Andersen, and H. R. Herschman.** 1994. v-*src* induction of the TIS10/PGS2 prostaglandin synthase gene is mediated by an ATF/CRE transcription response element. Mol. Cell. Biol. **14:**6531–6539.
67. **Xie, W., and H. R. Herschman.** 1995. v-*src* induces prostaglandin synthase 2 gene expression by activation of the c-Jun N-terminal kinase and the c-Jun transcription factor. J. Biol. Chem. **270:**27622–27628.
68. **Yuan, Y. L., and S. Fields.** 1991. Properties of the DNA-binding domain of the *Saccharomyces cerevisiae* STE12 protein. Mol. Cell. Biol. **11:**5910–5918.
69. **Yuan, Y. O., I. L. Stroke, and S. Fields.** 1993. Coupling of cell identity to signal response in yeast: interaction between the alpha 1 and STE12 proteins. Genes Dev. **7:**1584–1597.